



## Accepted Author Manuscript

**Journal:** *Journal of the Optical Society of America B*

**Article Title:** Flexible random lasers in dye-doped bio-degradable cellulose nanocrystalline needles

**Authors:** Gleice C. M. Germano, Yan D. R. Machado, Lucas Martinho, Susete N. Fernandes, Antonio Mario L. M. Costa, Edison Pecoraro, Anderson S. L. Gomes, and Isabel C. S. Carvalho

**Accepted for publication:** 11 November 2019

**Final version published:** 04 December 2019

**DOI:** <https://doi.org/10.1364/JOSAB.37.000024>

# Flexible Random Lasers in Dye-doped Bio-degradable Cellulose Nanocrystalline Needles

Gleice C. M. Germano<sup>a§</sup>, Yan D. R. Machado<sup>a§</sup>, Lucas Martinho<sup>a</sup>, Susete N. Fernandes<sup>b</sup>, Antonio Mario L. M. Costa<sup>c</sup>, Edison Pecoraro<sup>d</sup>, Anderson S. L. Gomes<sup>e</sup> and Isabel C. S. Carvalho<sup>a\*</sup>

<sup>a</sup> Physics Department, Pontifical Catholic University of Rio de Janeiro, Rio de Janeiro, 22451-900, Brazil

<sup>b</sup> i3N/CENIMAT, Department of Materials Science, Faculty of Science and Technology, Universidade NOVA de Lisboa, Campus de Caparica, 2829-516 Caparica, Portugal

<sup>c</sup> Department of Chemical and Materials Engineering, Pontifical Catholic University of Rio de Janeiro, Rio de Janeiro, 22451-900, Brazil

<sup>d</sup> Institute of Chemistry, UNESP -São Paulo State University, Araraquara, SP 14800-060, Brazil

<sup>e</sup> Physics Department, Universidade Federal de Pernambuco, Recife-PE, 50670-901, Brazil

§: Both authors contributed equally to this work

Corresponding Author: Phone/Fax +55 21 981331223

E-mail address: isabel.carvalho@puc-rio.br

Keywords: random laser, nanophotonics, nanocellulose

## Abstract

In this work, we developed and investigated a Random Laser based on Rhodamine6G (Rh6G) in ethylene glycol (EG) solution with varying cellulose nanocrystalline (CNC) needles as scatters in the lasing media. Besides the suspension-in-cuvette scheme, an alternative configuration was also employed: a dye-CNC flexible self-supported thick (70 $\mu$ m) film random laser made by drop casting of the CNCs+Rh6G+hydroxypropyl cellulose suspension. In relation to conventional scatters, the biodegradable cellulose nanocompounds showed a comparable reduction of both the spectral full width at half maximum and the energy threshold values, with an optimal concentration of 5mg [CNC]/ml[EG] in suspension. Its performance was also compared with other cellulose-based random lasers, presenting advantages for some parameters. The flexible film configuration shows similar results, but containing 10% less Rh6G than the suspension.

## Introduction

Cellulose based nanostructures have attracted a great deal of attention due to its increasing number of photonic applications in devices related to light generation, guiding, detection, amplification, and confinement [1–4]. Coherent emission cellulose based optical sources have been demonstrated in the form of random lasers. A Random laser (RL) is a low coherence photon source in which the optical feedback relies on scattering processes in nano or submicron structured media, instead of a conventional mirror-based Fabry-Perot cavity. RL has attracted a great deal of attention in the last decades, as reviewed in [5–7], after its first clear experimental demonstration in 1994 [8], over two decades after Lethokhov's theoretical proposal of such coherent light source [9]. Different gain media may be appropriately pumped to provide the required ingredients for laser emission, which include dyes, semiconductors, polymers, quantum dots, and rare earth ions [5]. The scattering media in the RLs are generally submicron or nanosized materials, either dielectric (TiO<sub>2</sub>, Al<sub>2</sub>O<sub>3</sub>), semiconductors (ZnO), rare earth doped glasses and nanocrystals (Nd, Er) or metallic nanomaterials (e.g. Au, Ag), in which case localized surface plasmons play an important role [5]. It is important to mention that random fiber lasers, whereby optical fibers are employed as the guiding media, have been demonstrated since 2007 [10], as reviewed in [11]. It is important to differ random fiber lasers [10,11], which employ the gain in the core of an optical fiber with embedded scattering medium, from random lasers based on fibers with nano or microstructures, such as in [12,13], which are themselves the scattering medium in the presence of a gain material.

Cellulose based random lasers were first reported in 2002 [14] and since then several publications have appeared [15–18]. It should be noticed that plasmonically enhanced RL based on cellulose matrices are reported in [16,17]. Table I summarizes the key features of those publications, including our results which will be discussed along the next sections. The threshold energy for the CNC+Rh6G liquid suspension was determined by experimental analysis and log-log graph for comparison with other literature works.

**Table I – Survey of cellulose based Random Lasers**

Ref	Scatterer ; Gain Medium	Solvent	$\lambda_{exc}(nm)$ ; $\tau_{exc}$	$\lambda_{em} (nm)$	$\Delta\lambda_{em} (nm)$	$E_{th}$
<i>This work</i>	CNC+ Rh6G	EG	532; 6ns	575	10	0.35mJ 0.075mJ <sup>(1)</sup>
<i>This work</i>	HPC + CNC; Rh6G	Flexible Thick Film	532; 6ns	575	10	0.30mJ
[12]de Oliveira et al	AC + PEO; Rh6G	DiCM; Meth	532; 6ns	570	8	97μJ
[18] Vasileva et al	TW; Rh6G	---	532; 4ns	---	5-6	0.7mJ
[17] Zhang et al	HPC + AuNP; Rh6G	Water	532; 30ps	553	---	4mJ/cm <sup>2</sup>
[16] Dos Santos et al	Flexible (BC) membrane + Si or AgNPs; Rh6G	Solid	532, 6ns	565	4-10	~0.70-2.5mJ <sup>(2)</sup>
[15] Viola et al.	Paper-Based + TiO <sub>2</sub> ; RhB	EG, Solid	532, 6ns	587-593	30	~0.01 - 0.1mJ <sup>(3)</sup>
[14] Lee, Lawandy	HPC + Kiton Red 620	Water	532, 7ns	639	5	25mJ, 41.5°C <sup>(4)</sup>

HPC - Hydroxypropyl Cellulose; CNC - Cellulose Nanocrystalline ; AC - Acetil Cellulose ; PEO - Polyethylene Oxide; EG - Ethylene Glycol; DiCM - Dichloromethane; Meth - Methanol; BC - Bacterial Cellulose; TW - Transparent Wood;  $\lambda_{exc}$ - excitation wavelength;  $\tau_{exc}$ - laser excitation pulse width;  $\Delta\lambda_{em}$ - FWHM;  $E_{th}$ - energy threshold.

<sup>(1)</sup>Value from log-log graph

<sup>(2)</sup>Depending on NP concentrations

<sup>(3)</sup>Depending on paper circuitry

<sup>(4)</sup>Temperature depending threshold

Among the studied cellulose based materials, cellulose nanocrystals are especially interesting due to their mechanical strength, flexibility and bio-compatibility, associated with its low cost and eco-friendly fabrication processes [3,4].

In this work, we report on alternative random lasers schemes based on a dye embedded in cellulose nanocrystalline (CNCs) needles as the scattering medium, in suspension, in a liquid or in a flexible 70  $\mu\text{m}$  thick hydroxypropyl cellulose (HPC) film with CNCs.

## Materials and Methods

### Materials

The CNCs were produced from microcrystalline cellulose from cotton, as reported in [4]. The resultant aqueous CNC suspension (with  $3.2\pm 0.3$  wt.% CNC content determined by gravimetric method) was diluted to 0.5 wt.% CNC content and freeze-dried directly (Zirbus, VaCo 2). The resulting white flakes are composed of multiple CNCs, as can be seen in Figure 1a.

To obtain the CNC liquid suspension, different amounts of CNCs were added to 2.0 ml of ethylene glycol (EG) (Reagen 99.6%) resulting in a final concentration of CNCs of 1, 3, 5 and 7mg/ml respectively, and kept under intense sonication (130 Watts, Sonics Vibra-Cell CV18) for three 5 minute sessions until complete dispersion. Afterwards, 200  $\mu\text{l}$  of a solution of RH6G (10mM in ethylene glycol) were added to the CNC suspensions. In order to obtain a homogeneous suspension the final mixtures were put in ultrasonic bath (Ultracleaner 700) for 5 minutes.

To obtain the solid film suspensions 0.22g of HPC (Sigma Aldrich 99%, average MW 100.000) and 1.0 mg of CNC were added to 2.0 ml of distilled water and then sonicated (130 Watts, Sonics Vibra-Cell CV18) for three 5-minute sessions for complete dissolution of HPC. Afterwards, 100 $\mu\text{l}$  of a solution of RH6G (4mM in ethylene glycol) was added to the HPC ultrasound bath (Ultraclear 700, 50kHz) for 5min. The final suspensions were drop casted on polypropylene molds with 3.5cm x 2.0 cm and dried in an oven at 60  $^{\circ}\text{C}$  for ~1hr, forming a film with 70 $\mu\text{m}$  thickness. The random laser emission measurements were made right after the drying process.

As ethylene glycol (EG) has a higher viscosity when compared to methanol, the EG was used here which allowed the dispersion of a higher concentrations of CNCs in the suspension [19]. Also, there is an influence on the threshold energy by the refractive index of the solvent, as the EG refractive index (1.43) is higher than the methanol refractive index (1.33). It is expected a higher energy threshold for the suspension using EG as a solvent [20].

### SEM Characterization - CNC needles

In order to confirm the average dimensions of the CNCs, droplets of aqueous suspension of 0.01 wt% CNCs were deposited onto aluminum stubs and coated with thin carbon layer (produced with a Q150T ES Quorum sputter coater). The images of CNCs flakes were acquired with JEOL JSM 6701F (SEM-FEG) and the images of individual CNCs with a Carl Zeiss Auriga crossbeam (SEM- focus-ion-beam (FIB)) workstation instruments, operated at 2kV and 5 kV, respectively. ImageJ software (version 1.45 s) was used to measure these entities and values of  $135\pm 48$  nm and  $4\pm 1$  nm for particles' length and diameter, respectively, were determined for a total 160 measurements for each dimension.

Shown in Fig. 1 are the images obtained with a SEM-FEG and SEM-FIB, presenting the morphology of the CNCs as in flakes (macro size agglomerates) (Fig. 1a) and as individual needles (Fig. 1b).

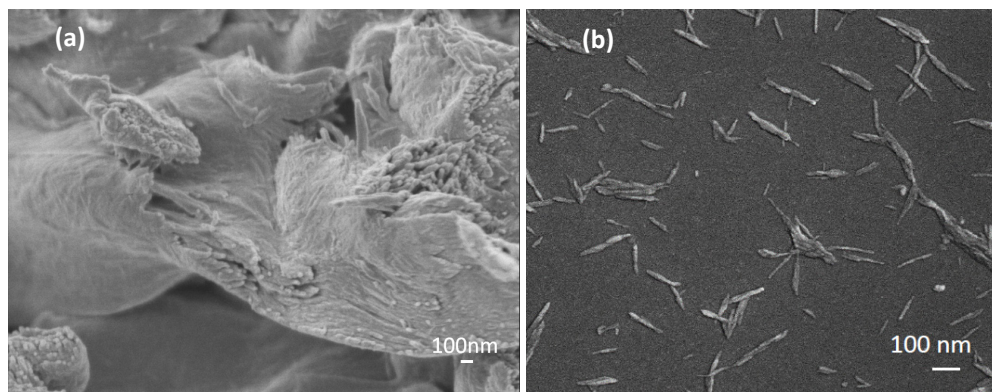


Fig. 1: Images obtained by SEM-FEG of the (a) CNCs as in flakes (macro size agglomerates) cross section and (b) of the needles.

The CNC presents flakes which are formed by nanofibrillated cellulose made according to ref [4]. In the CNC flakes, the needles, stack up in a self-organized form. In Fig. 1a it is also observed the needles, from a stacking of the fibrillated cellulose, clearly emerging from a cross section of the sample. The needles are the scattering centers of the random laser, providing sufficient optical feedback for its operation and high efficiency.

### HPC+CNC Films

The polarized optical microscopy images (LeicaDM2500 Optical microscope) (Fig. 2) show no evidence of CNC clustering for both systems, *i.e.*, HPC and HPC+CNC films, which could influence on the results of random laser emission. If it were so, polarized light domains will arise from the images, no matter if in the macroscopic or microscopic scale, as observed before in the literature. For instance, in ref [4] a hierarchical self-organized cholesteric structure of CNC is observed in pure CNC dried films. In this sense, no such structures were observed for HPC and HPC+CNC films under polarized light, as depicted on the digital photographs and optical micrographs figures (Fig.2).

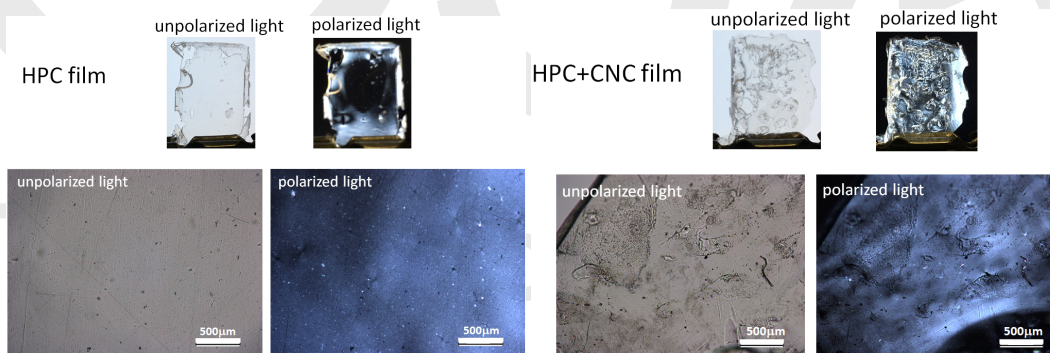


Fig. 2: Digital photographs and light polarized optical micrographs of HPC and HPC+CNC films.

The light contrast found in optical microscopy under polarized light for both films is due to the intrinsic birefringence of such composites. Although the films are transparent for visible light, the birefringence emerges as consequence of the presence of two phases with different refractive indexes.

The light polarized optical microscopy data show that there is no hierarchical clustering of the CNC in the HPC films. However, that does not mean the distribution of the CNC needles is totally random. FEG-SEM images of the HPC+CNC films cross-section (Fig.3) show the needles mostly are aligned as stacked layers along the longitudinal axis of the film. The images in Fig.3 were acquired with JEOL JSM 7100FT (SEM-FEG). From the macro scale, such tendency could be pondered as a long range morphological organization. Nevertheless, we do not view such organization as a factor, which could have influence on the random laser emission properties, once it is not a localized organization.

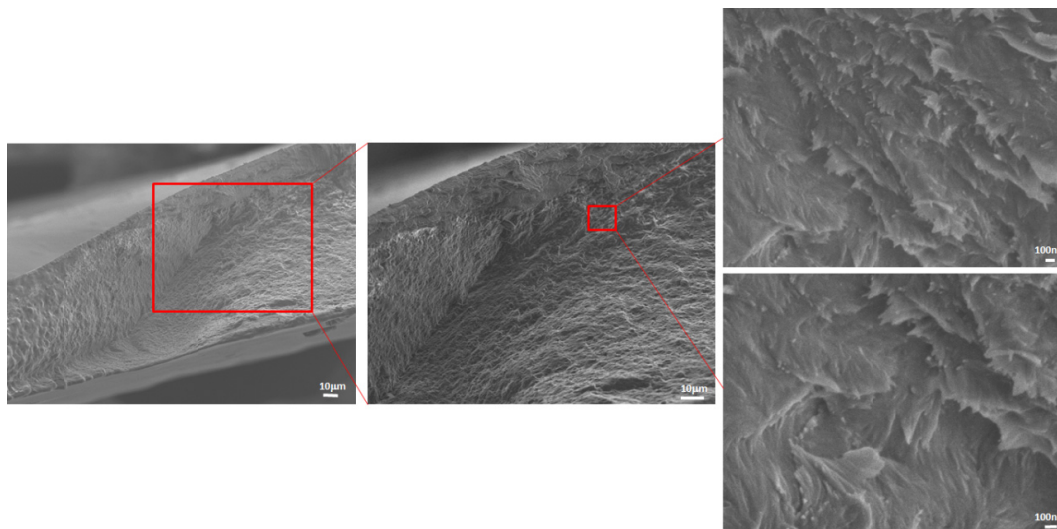


Fig.3: FEG-SEM micrographs of HPC film containing 5mg/mL of CNC.

## Random Laser Characterization

The lasing emission spectra of the CNCs+Rh6G suspension and the CNC+Rh6G-on-thick film were measured upon excitation with a pulsed Q-Switched Nd: YAG laser (Brio - Quantel, 10 Hertz, 6ns,  $\lambda = 532$  nm). The pump beam carrying a maximum energy of 9mJ and with a 2.1 mm beam diameter was launched on the sample. A 75mm convex lens was used to collect the random laser emission and direct onto the spectrometer. The spectral analysis was performed with an Ocean Optics USB4000-UV-VIS spectrometer (spectral resolution  $\sim 1.5$  nm). The measurements of all samples were recorded under identical experimental conditions and carried out at room temperature. Figure 4 shows the experimental setup, the inset shows images of the NCC+Rh6G suspension in the cuvette and in the HPC flexible film.

The excitation light was directed onto the sample in the quartz cuvette at a  $45^\circ$  angle to avoid creating a Fabry-Perot cavity due to reflections on the (10mm x 10mm) cuvette walls. Although internal cavities were not easy to excite in the thick film, the same excitation angle geometry was maintained.

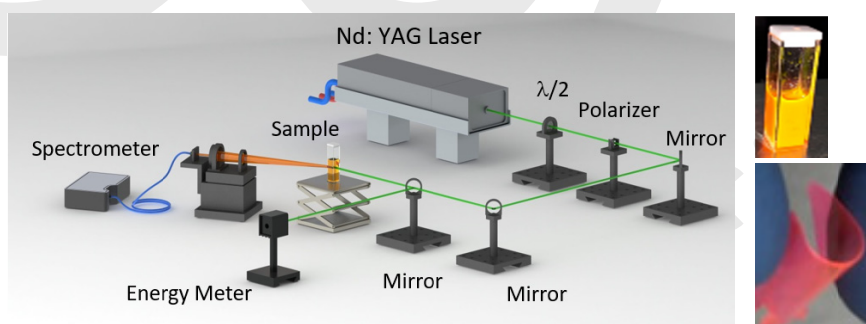


Fig. 4: Experimental setup for the CNC+Rh6G suspension in the cuvette and in the HPC thick film random laser characterization. The inset shows images of the samples.

## Results on Random Laser Behavior

### *CNCs+Rh6G suspension*

The RL emission from the CNCs+Rh6G suspension is evidenced by a spectral narrowing for samples under different excitation energies (Fig.5). For all the samples, the linewidth is strongly reduced from 60nm to 10nm at its full width at half maximum (FWHM), from below to well above the threshold for

various cellulose concentrations. In the inset of Fig 5, the narrowing does not occur through the entire spectral emission, but a broad pedestal is still observed for excitation pulse energies above the threshold.

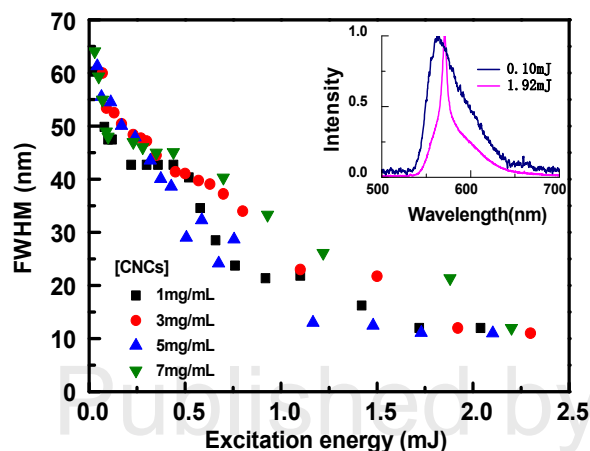


Fig.5: FWHM of the CNC+Rh6G suspension spectra emission upon laser excitation as a function of excitation energy for samples with different CNC concentrations. The inset shows an emission spectra for well below (blue curve) and above (pink curve) threshold energy.

The emitted intensity was affected by the incorporation of more CNCs to the suspension, which in turn affects the scattering in the random laser media. Fig. 6, shows the emission intensity in a log-log plot in order to reveal the response of the RL for the various CNC's concentration. As can be seen in Fig.6 inset, for 5mg/ml CNCs the random laser efficiency greatly improves with a threshold of 0.35mJ, which corresponds to 50% of the energy threshold for the sample with 1mg/ml CNC. Therefore, the 5mg/ml is the optimal concentration when compared with the 1mg/ml, 3mg/ml and 7mg/ml concentrations. Also, increasing the CNCs amount above 5mg/ml increases the threshold value, reducing the laser efficiency.

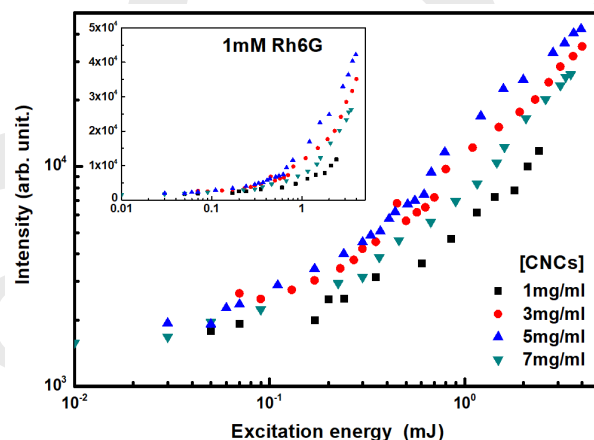


Fig. 6: Random laser emitted intensity as a function of the excitation energy for various CNC concentrations. The inset is a log-linear plot of the emitted intensity as function of the excitation energy for various CNC concentrations.

### HPC+CNC+Rh6G Flexible Random Laser

The self-supported flexible HPC+CNC+Rh6G RL was characterized and compared with the CNC+Rh6G suspension RL. The results for the linewidth reduction and emitted intensity as a function of input power are shown in Figure 7 (a) and (b). It should be noted that the film samples have 10% less CNCs needles than in the suspension format, although the energy threshold (0.3mJ) is similar. Also, the excitation energy for the film sample was increased only up to 1mJ, due to the degradation of the sample above this energy.

It is important to emphasize that the self-supported film configuration offers more flexibility and the RL operates with no feedback from any solid substrate. Such condition and based on the physical-chemical properties of the start suspension used to casting the films, *e.g.* viscosity and colloidal stability, allow us to ponder the potential of such system in manufacturing lab-on-chip fluorescent biosensors. A film as such, could replace bulk diodes, usually found in fluorescence based detection biosensors devices [21].

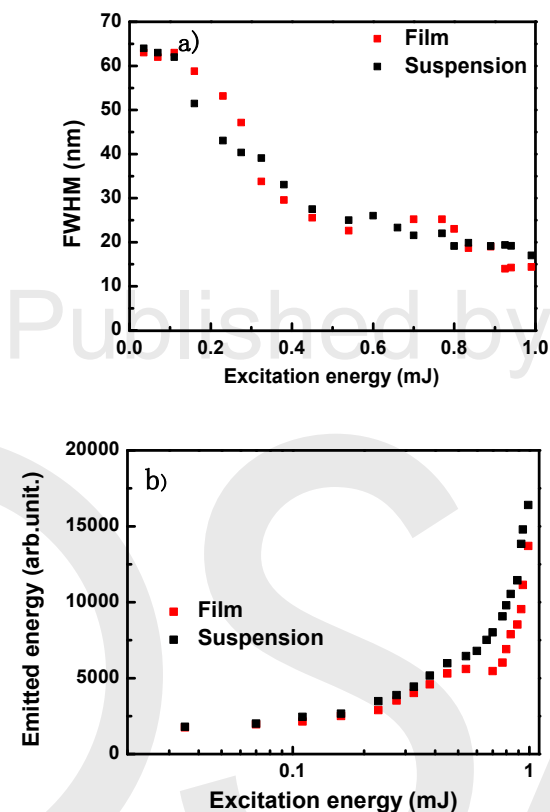


Fig.7 - a) FWHM (a) and (b) Emission intensity as function of the excitation energy for the HPC+CNCs+Rh6G suspension (black square) and thick film (red square). The CNCs thick film and suspension concentrations are 0.5mg and 10mg, respectively, for the same 4mM of Rh6G dye concentration.

The concentration of CNCs in the solid suspension was  $10.2\text{mg}/\text{cm}^3$  and in the liquid suspension the CNC concentrations were 1, 3, 5 and  $7\text{mg}/\text{cm}^3$ . Also, the Rhodamine6G concentration in the solid suspension was  $4.92 \times 10^{18}$  molecules/ $\text{cm}^3$  and in the liquid suspension  $5.47 \times 10^{17}$  molecules/ $\text{cm}^3$ . Therefore, the concentration of both CNCs and Rh6G is higher in the solid than in liquid suspensions. On the other hand, in the thick HPC film the laser beam interacts in a smaller optical path when compared to the path in the cuvette (1cm x 1cm). This reduces the intensity of the Rh6G emission considerably, demonstrating the good scattering properties of the HPC + CNC film since it has the same threshold value as in the liquid suspension. It was observed that the HPC+Rh6G film has a pink color, which can be associated to a shift at the peak maximum of its absorption band, with respect to the monomer peak position. Such shift indicates the formation of J-type aggregates. On the liquid suspension it presents the Rh6G characteristic orange color and by the absorption spectrum measurement one can conclude that, besides Rh6G monomers, two types of aggregates occur, *i.e.*, H and J-type aggregates [22], which leads to a less intense emission. One concludes that for the same threshold energy the self-supported flexible film needs a shorter optical path and does not favor the formation of both H and J-type aggregates, thus allowing different applications as will be discussed in the conclusion.

## Discussion

Our results using the novel bio-degradable CNC needles as the scatters for a dye-based RL can be directly compared to other literature results also using cellulose based scatters, as summarized in table I. Except for the work of ref. 17, which employs 30ps pulses, all the other tabulated works employ 532nm/4-7ns long pulses. The lasing bandwidth of all reported RLs are around the same value between 4-10nm, except for the work of ref. [15] (30nm). In RLs, the bandwidth is determined by the gain medium, which in the case of dyes can vary according to the used solvent and excitation wavelength. Therefore, this characteristic is similar among all reported cellulose RL including ours. The central emission wavelength follows the same analysis as above. Therefore, except for Kiton Red 620 (emission around 640nm) all the other rhodamine based RL had peak wavelength between 553nm and 593nm. Another important parameter is the RL threshold. The threshold value in our work is among the smaller threshold values shown in table I. On the other hand, in reference [12] where an electrospun polymeric composite was investigated, it is presented a threshold energy smaller than all tabulated work, this fact can be attributed to a higher dye + scatters concentrations and a lower solvent refraction index, which directly affect the threshold energy as discussed in reference [20]. Moreover, for a fluidic paper-based device, this configuration leads to a lower energy threshold [15].

Finally, it should be mentioned that an important and detrimental characteristic of the organic based RL is the operating lifetime under pumping regime. The degradation of the random laser in the thick film configuration was performed by evaluating the variation of the FWHM and the intensity as a function of the number of shots at a known frequency (5Hz), using the software SpectraSuite 1.6.0\_11. The degradation time in our dye-based RL system was similar to other reported in the literature (several 10's of minutes) [ [23] and refs therein]. This can be mitigated or overcome using solid state gain media, such as rare earth doped nano/sub-micron particles [24] or semiconductor based nano or micron sized structures [25].

## Conclusion

In this work, we have investigated two architectures for a random laser using various concentrations of CNCs needles as scatters and Rh6G as the gain medium. From the suspension-in-cuvette architecture, an optimized CNC concentration of 5mg/ml was obtained. We also investigated the random laser in a flexible, self-supported 70  $\mu\text{m}$  thick film formed by HPC containing CNCs+Rh6G. The films presented a similar energy threshold when compared to the colloidal suspension, but with 10% less Rh6G than the suspension. Such results point out to the potential of such system in manufacturing lab-on-chip fluorescent biosensors, replacing, for instance, bulk diodes usually found in fluorescence based detection biosensors devices. Both designs were compared to reported literature work on cellulose based RLs, with a very good comparative performance.

## Acknowledgments

This work was partially supported by the Brazilian agencies FINEP, CAPES, FACEPE, CNPq and Instituto Nacional de Fotônica – INFo. I.C.S.C. and A.S.L.G. acknowledge support by the Office of Naval Research Global. The authors thank Prof M. Helena Godinho for the CNC material and for fruitful discussions. It was also funded by FEDER funds through the COMPETE 2020 Program, National Funds through FCT - Portuguese Foundation for Science and Technology and POR Lisboa2020, under the projects with references POCI- 01-0145-FEDER-007688 (Reference UID/CTM/ 50025), UID/BIA/00329/2013, PTDC/CTM-BIO/6178/2014, M-ERA- NET2/0007/2016 (CellColor) and PTDC/CTM-REF/30529/2017(NanoCell2SEC). I.C.S.Carvalho acknowledges Mr Fredy G. O. Gutiérrez for technical support. The authors are grateful to CBPF for the use of the facilities for electron microscopy in the LabNano/CBPF, Rio de Janeiro-BR (JEOL JSM-7100FT), the laboratory VDG-PUC-Rio for the use of the facilities for electron microscope SEM-FEG JEOL JSM6701F.

## Disclosures

The authors declare no conflicts of interest

## References

1. R. J. Moon, A. Martini, J. Nairn, J. Simonsen, and J. Youngblood, "Cellulose nanomaterials review: structure, properties and nanocomposites," *Chem. Soc. Rev* **40**, 3941-3994 (2011).
2. S. Caixeiro, M. Peruzzo, O. D. Onelli, S. Vignolini, and R. Sapienza, "Disordered Cellulose-Based Nanostructures for Enhanced Light Scattering," *ACS Appl. Mater. Interfaces* **9**, 7885-7890 (2017).
3. D. Gaspar, S. N. Fernandes, A. G. De Oliveira, J. G. Fernandes, P. Grey, R. V. Pontes, L. Pereira, R. Martins, M. H. Godinho, and E. Fortunato, "Nanocrystalline cellulose applied simultaneously as the gate dielectric and the substrate in flexible field effect transistors," *Nanotechnology* **25**,094008, 1-11 (2014).
4. S. N. Fernandes, P. L. Almeida, N. Monge, L. E. Aguirre, D. Reis, C. L. P. de Oliveira, A. M. F. Neto, P. Pieranski, and M. H. Godinho, "Mind the Microgap in Iridescent Cellulose Nanocrystal Films," *Advanced Materials* **29**, 1603560,1-7 (2017).
5. F. Luan, B. Gu, A. S. L. Gomes, K. T. Yong, S. Wen, and P. N. Prasad, "Lasing in nanocomposite random media," *Nano Today* **10**, 168-192 (2015).
6. L. Sznitko, J. Mysliwiec, and A. Miniewicz, "The role of polymers in random lasing," *Journal of Polymer Science, Part B: Polymer Physics* **53**, 951-974 (2015).
7. S. F. Yu, "Electrically pumped random lasers," *Journal of Physics D: Applied Physics* **48**, 483001,1-28 (2015). S F
8. N. M. Lawandy, R. M. Balachandran, A. S. L. Gomes, and E. Sauvain, "Laser action in strongly scattering media," *Nature* **368**, 436-438 (1994).
9. V.S. Lethokhov, "Generation of lighth by a scattering a medium with a negative resonance absorption.," *Sov.Phys.JETP*. **40**, 835-840 (1968).
10. C. J. S. De Matos, L. De S. Menezes, A. M. Brito-Silva, M. A. Martinez Gámez, A. S. L. Gomes, and C. B. De Araújo, "Random fiber laser," *Physical Review Letters* **99**, 153903, 1-4 (2007).
11. D. V Churkin, S. Sugavanam, I. D. Vatnik, Z. Wang, E. V Podivilov, S. A. Babin, Y. Rao, and S. K. Turitsyn, "Recent advances in fundamentals and applications of random fiber lasers," *Advances in Optics and Photonics* **7**, 516-569 (2015).
12. M. C. Albuquerque de Oliveira, L. de Souza Menezes, P. I. R. Pincheira, C. Rojas-Ulloa, N. R. Gomez, H. P. de Oliveira, and A. S. Leônidas Gomes, "A random laser based on electrospun polymeric composite nanofibers with dual-size distribution," *Nanoscale Advances* **1**, 728-734 (2019).
13. G. Lv, D. Huang, S. Wu, G. Ren, W. Yang, and T. Li, "Random lasing action generation in polymer nanofiber with small diameters," *Laser Physics* **28**, 075803,1-6 (2018).
14. Kijoon Lee and N. M. Lawandy, "Laser action in temperature-controlled scattering media," *Optics Communications* **203**, 169-174 (2002).
15. I. Viola, N. Ghofraniha, A. Zacheo, V. Arima, C. Conti, and G. Gigli, "Random laser emission from a paper-based device," *Journal of Materials Chemistry C* **1**, 8128-8133 (2013).
16. M. V. Dos Santos, C. T. Dominguez, J. V. Schiavon, H. S. Barud, L. S. A. De Melo, S. J. L. Ribeiro, A. S. L. Gomes, and C. B. De Araújo, "Random laser action from flexible biocellulose-based device," *Journal of Applied Physics* **115**, 083108,1-5 (2014).
17. R. Zhang, S. Knitter, S. F. Liew, F. G. Omenetto, B. M. Reinhard, H. Cao, and L. Dal Negro, "Plasmon-enhanced random lasing in bio-compatible networks of cellulose nanofibers," *Applied Physics Letters* **108**, 011103, 1-4 (2016).
18. E. Vasileva, Y. Li, I. Sychugov, M. Mensi, L. Berglund, and S. Popov, "Lasing from Organic Dye Molecules Embedded in Transparent Wood," *Advanced Optical Materials* **5**,1700057,1-6 (2017).
19. L. Yang, G. Feng, J. Yi, K. Yao, G. Deng, and S. Zhou, "Effective random laser action in Rhodamine 6G solution with Al nanoparticles," *Applied Optics* **50**, 1816-1821 (2011).
20. J. Yi, G. Feng, L. Yang, K. Yao, C. Yang, Y. Song, and S. Zhou, "Behaviors of the Rh6G random laser comprising solvents and scatterers with different refractive indices," *Optics Communications* **285**, 5276-5282 (2012).
21. N. M. M. Pires, T. Dong, U. Hanke, and N. Hoivik, "Recent developments in optical detection technologies in lab-on-a-chip devices for biosensing applications," *Sensors (Switzerland)* **14**, 15458-15479 (2014).
22. M. Lofaj, I. Valent, J. Bujdák , " Mechanism of rhodamine 6G molecular aggregation in montmorillonite colloid", *Central Eur. J. of Chem.* **11** (10) ,1606-1619 (2013) .

23. P. I. R. Pincheira, A. F. Silva, S. I. Fewo, S. J. M. Carreño, A. L. Moura, E. P. Raposo, A. S. L. Gomes, and C. B. de Araújo, "Observation of photonic paramagnetic to spin-glass transition in a specially designed TiO<sub>2</sub> particle-based dye-colloidal random laser," *Optics Letters* **41**, 3459–3462 (2016).
24. A. L. Moura, L. J. Q. Maia, A. S. L. Gomes, and C. B. de Araújo, "Optimal performance of NdAl<sub>3</sub>(BO<sub>3</sub>)<sub>4</sub> nanocrystals random lasers," *Optical Materials* **62**, 593–596 (2016).
25. M. L. da Silva-Neto, M. C. A. T. Dominguez, R. E. M. Lins, N. Rakov, C. B. de Araújo, L. de S. Menezes, H. P. de Oliveira, and A. S. L. Gomes, "UV random laser emission from flexible ZnO-Ag-enriched electrospun cellulose acetate fiber matrix," *Sci Rep* **9**, 11765,1–9 (2019).

Published by

OSA<sup>®</sup>

The Optical Society